A Technical Study of Five Ruby Ambrotypes

Lisa M. Duncan
Winterthur/ University of Delaware Program in Art Conservation
August 9, 2009

ABSTRACT- Ruby ambrotypes are images made photographically upon a colored glass support. A descriptive study of ruby ambrotypes was carried out on five samples. Goals of analysis included identifying the colorants in the glass support, classifying coatings on the surface and characterizing tarnish. Elemental analysis performed with x-ray fluorescence (XRF) spectroscopy and scanning electron microscopy-energy dispersive spectroscopy (SEM-EDS) revealed the presence of manganese as the colorant in the glass. Surface coatings were found to be complex mixtures of natural resins and fatty acids using Fourier transform infrared (FT-IR) spectroscopy in tandem with gas chromatography-mass spectrometry (GC-MS). Tarnish of the silver image was identified with Raman spectroscopy and SEM-EDS with backscattered electron (BSE) imaging to be a combination of predominantly silver sulfide and silver chloride salts.

1. INTRODUCTION

1a. Overview

A technical study of ruby ambrotypes was undertaken to understand more about how these images were made and how they have deteriorated over time. This study should incite further research in these complex objects and inform future treatment decisions in art conservation.

1b. Identification of an ambrotype

Ambrotypes were popularly produced in America in the decade just before the Civil War. The *common ambrotype* is a wet collodion process produced on a clear glass support. Refer to Figure 1 for a visual interpretation. During exposure of an ambrotype plate in a camera, image highlights receive greater light and become opaque in development. The shadows receive little or no light exposure and are transparent. The image is a negative that when viewed with a black backing becomes a positive.

Historically, there were a number of options for preparing the dark backing. One type of backing was coated directly on the glass with a black pigmented Canada balsam or pigmented asphaltum called "black varnish." Sometimes the "black varnish" was applied over the collodion image and viewed through the glass support. Also, backings could be separate from the glass. They were made of black paper, dark velvet or Japanned-tin plates. Figure 2 is a cross section illustration of the common ambrotype. Moor (1976) presents a complete description of variations in the ambrotype presentation.
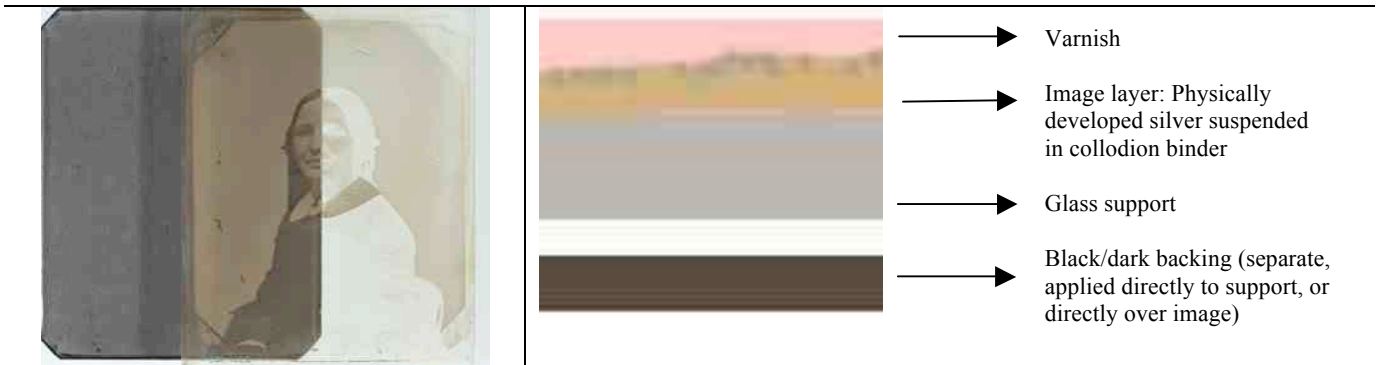
	 Varnish Image layer: Physically developed silver suspended in collodion binder Glass support Black/dark backing (separate, applied directly to support, or directly over image)
Figure 1: The common ambrotype plate half removed from backing to expose a negative image in transmitted light	Figure 2: Cross section illustration of a common ambrotype

The making of ambrotypes upon a colored glass support started about 1854 in England, and 1856 in America. In reviewing the American published Humphrey's Journal, H. Draper submitted the earliest entry describing the use of colored glass for ambrotypes on October 1, 1856. The dark glass dually provided a support for the image and a dark backing.

Anthony's Invention and Improvement catalog from 1857 heralded the sale of colored glass by stating, "the colored glass meets a want that has been long felt by Ambrotypists. Made expressly for this purpose at the request of some of the most eminent Ambrotypists."

Today ambrotypes on a colored glass are referred to as *Ruby ambrotypes* or *ambrotypes on Bohemia glass*. When viewing a ruby ambrotype in transmitted light, the colored glass is evident. Most often the color of the glass was reddish to purplish-black in color but there are known samples on green, amber or blue glass. (Osterman, 2007) Figures 3 & 4 elucidate a ruby ambrotype in transmitted light and a cross section illustration.
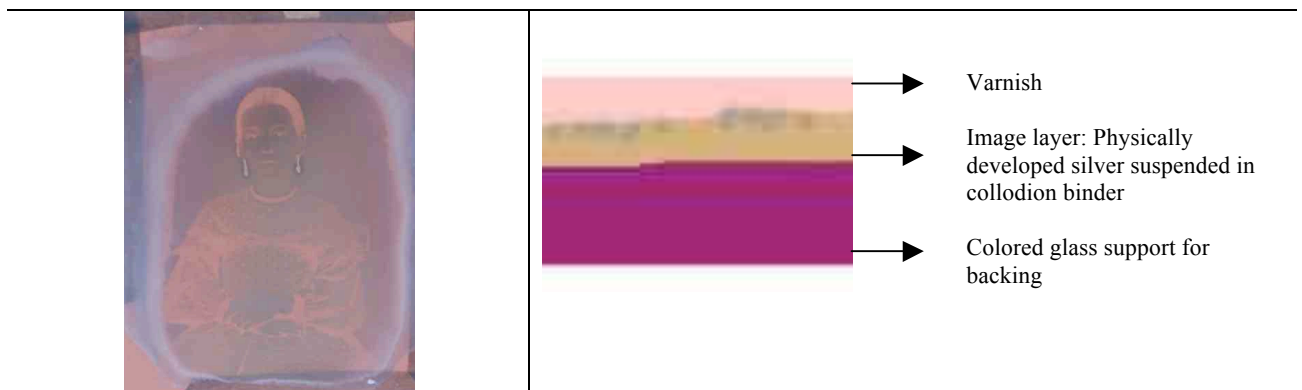
	 Varnish Image layer: Physically developed silver suspended in collodion binder Colored glass support for backing
Figure 3: The negative image and colored glass of a *ruby ambrotype* when viewed with transmitted light	Figure 4: Cross section illustration of a *ruby ambrotype*.

1c. Historical background

The Englishman Frederick Scott Archer introduced the wet plate collodion negative on glass to the photographic societies in the March 1851 issue of the *The Chemist*. One application of Archer's findings was the ambrotype. He described the use of collodion on a glass plate to make a negative of better clarity and quality to the calotype paper negatives of the day. He did not patent his findings making the technique more available to the public.

The word *ambrotype* was not applied to the process until James Cutting's series of patents from the year 1854 in America. (Osterman, 2007) In his patents (#11213, #11266 & #11267 (Schimmelman, 2002)), Cutting described a sealing technique for *ambrotypes* and coined the term (with the help of M. Root) from the Greek word for "imperishable." During the time period a more common name for the process would have been *daguerreotypes without reflection*, *daguerreotypes on glass*, *collodion positives on glass, verreotypes*, *positive pictures on glass*, or simply *collodion positives*. (Osterman, 2007)

The Cutting patent outraged many photographers who were already working within the medium. (Newhall, 1958) They felt he had received a patent for a process that he had not invented. By the mid 1850s, there were already many practioners of the ambrotype process. Itinerant artists were traveling around the country taking portraits in towns and then moving on. Many daguerreotypists of the day had picked up the new technique, stopping production of the daguerreotype all together. The ambrotype was a cheaper means of producing a portrait likeness and could be sold more readily to customers.

The ambrotype was made in sizes similar to the daguerreotype (ninth, sixth, quarter, half, full plate). They were often housed in cases and bound into packages identical to the daguerreotype. Some customers of the time could not distinguish between the two processes. By 1862 and the start of the Civil War in America, the ambrotype process was obsolete. (Newhall, 1958) It had been almost completely replaced by the Ferrotype, a wet collodion process applied to a Japanned iron support. In other parts of the world, the ambrotype enjoyed longer commercial popularity.

1d. Wet Collodion Process & Materials

The binder for the silver particles in the ambrotype is collodion. Collodion was introduced to the public by the medical profession in 1846 for mending wounds. The term collodion comes from the Greek word meaning *to stick*. It is a less nitrated cellulose nitrate and made when cotton is treated with nitric and sulfuric acid. It degrades, becoming nitrated. Hydroxyl groups and one hydroxymethyl group can be substituted with nitrate groups on the D-glucose in the β-pyranose form. (McGlinchey & Maines, 2005) The fully substituted material is named *gun cotton* and is not soluble in ethers or alcohols. Alternately the less nitrated

collodion, also called peroxylin in historic texts, was effectively soluble in ethers and alcohols. Refer to Figure 5 for a structure of collodion.
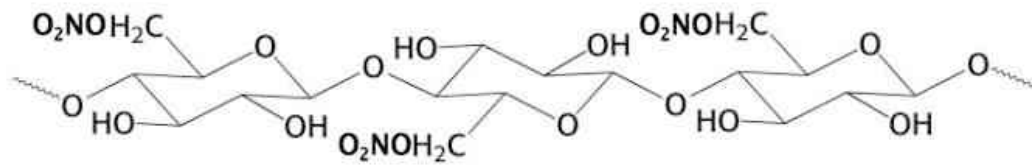

Figure 5: Collodion

The process of coating, sensitizing, exposing, developing, and fixing the ambrotype was done while the collodion binder was wet and known as a *wet plate* method. An ambrotype was made when salted collodion containing iodides and bromides (bromides were introduced later and allowed the sensitivity into the green region of light), were poured over a polished piece of plate or window glass.

The plate was sensitized in a bath of silver nitrate, and exposed in a camera. Often the image was underexposed to produce a lighter image. They were developed in ferrous sulfate, and fixed in sodium thiosulfate or potassium cyanide. The plate was washed and then often varnished to protect the image from damage during handling. In certain circumstances, mercuric chloride was used to whiten the highlights and give a more desirable positive image. (Osterman, 2007) The bleaching was later deemed unnecessary when iron sulfate was adopted as the developer with a potassium cyanide fixer.

The image material in an ambrotype was physically developed silver. This is created when a latent image was produced and intensified with a developer. The silver particles were small enough to be discernable with the help of a transmission electron microscope. (Reilly, 1986) The particles were round and scatter light to visually appear tan in tone.

1e. *Coatings applied to ambrotypes*

Most photographers of the 1850s purchased varnishes ready-made from photographic catalogs. They also made their own, following recipes outlined in treatises of the time and photographic journals. Varnishes were usually natural resins dissolved in alcohols or turpentine but could have easily been polysaccharides, waxes, or proteins. (McCabe et al, 2005)

The purpose of varnishes on ambrotypes was to provide a protective coating that would help preserve the image. An important characteristic of coating materials was the transparency, because they were applied directly over the image. Clara von Waldthausen has compiled a comprehensive list of varnishes used on photographs which she collected from primary sources. She identified the use of white wax, soft copal, sandarac, yellow and white lac, melted amber, essence of turpentine, gum sandarac, gelatin, shellac, gum Arabic, Venice turpentine, mastic, and dammar on collodion processes. Burgess (1858) describes the use of copal, gum-dammar,

shellac and copal varnishes for use on ambrotypes. Additionally, McCabe (1991) reported the use of varnishes composed of triterpenes in tandem with alcohols for wet-plate negatives. A recent publication edited by McCabe et al (2005) provides an excellent reference for coatings on photographs.

McCormick-Goodhart (1989) reported studies of Fourier Transform infrared (FT-IR) spectroscopy in transmission mode to characterize varnishes on wet-plate negatives. By removing microgram samples and running them in transmission mode, he found shellac and sandarac resins. McCormick-Goodhart (1990), also studied varnishes on ferrotypes and found a bleached shellac coating used on these particular objects. Perron (1989) succeeded in characterizing photographic materials with FT-IR used in reflectance mode to eliminate destructive sampling.

1f. *Past studies of silver tarnish*

Understanding the deterioration of silver image has fascinated photographers, conservators, and scientists alike since photography was invented. An image will begin to react with the surrounding environment immediately after creation. Most reports about silver tarnish come from literature on silver objects. Analysis in relation to photography has been less studied. Hatchfield (2005) and Stambolov (1966) provide insightful and general explanations of silver deterioration mechanisms and environmental impacts on collections. There have been studies within the field of photographs by Swan (1979), Barger (1984), Daffner (1996) and Di Pietro (2002), among others, who discuss deterioration of the silver image of glass plate negatives and daguerreotypes. All alluded to sulfides as the predominant cause of tarnishing. Most recently Centano et al. (2008) discussed the use of Raman spectroscopy to characterize a white crystal on the surface of daguerreotypes as silver chloride. Haist (1979), Weaver (2007) and articles published by James Reilley et al. at the Image Permanence Institute (IPI) also provide insight on image deterioration of paper-based photographs.

Scanning electron microscopy-energy dispersive spectroscopy (SEM-EDS) has been utilized to look at cased objects and also photographs on a paper support. The author is not aware of any reports on silver tarnish on ambrotypes. McCormick-Goodhart (1990) has also used it to analyze ferrotypes and Swan (1979) used it for daguerreotypes. Barger (1982) also provides SEM imaging of daguerreotypes in research to define terminology for deterioration. Additionally, Penichon (1999) used SEM-EDS to identify the elements found in toned collodion paper-based prints.

1g. *Colored glass for ambrotypes*

Historical background. A photographic text described the colored glass used in ambrotypes as the "finest quality of a medium thick plate glass" (Burgess, 1857), although it is likely that a photographer used whatever materials were available. A lower quality glass called *common glass* or *window glass,* with bubbles and striations, was also used. Most photographers bought their glass pre-cut from photographic warehouses in New York and Philadelphia. In a personal discussion with M. Osterman (2007), he believes that warehouses likely purchased the ambrotype glass from stained window glass manufactures.

By the 1800s there was no longer a need to purchase glass from Europe. Lloyd (1963) describes the first noted production of red glasses in America around 1840. Glass production in America often began in areas rich in coal and sand, both required materials for mass production. A company in Pittsburgh, PA imported German glass craftsman in 1827 and began producing a "Pittsburgh Ruby" glass sold as "true Bohemian" (Lloyd, 1963). The Morris Company, located in Manhatten, also began production of stained glass around 1837. A big market for colored glass, especially red, was for lights and decoration on steamboats floating up and down the Hudson River.

A merchant could find window glass almost anywhere by the mid-19th century. Home building in the 1840's was used stained glass. Colorful glass was integral to Gothic revival architecture of the day.

Stained window glass manufacture. Stained glass is a *pot-metal glass*, usually made when metal oxides or suspended metal colloids in a molten stock glass. (Sloan, 1993) The plate is formed in a number of ways including cylinder glass and cast glass. One is described as cylinder glass (also called muff or antique glass). This procedure involves blowing glass in a tube. By the mid-nineteenth century a hand pump was used to supply airflow. The bottom was opened to make a cylinder and the tube sliced lengthwise. The tube is opened up and annealed to relax the shape into a plate.

Casting and polishing with hydropower could also make glass, producing a higher quality product, void of streaks. The sizes of plate glass could be manufactured at sizes exceeding 80 inches by 160 inches. (Roth, 1971) The colored sheet glass was made by forcing molten glass through rollers and was referred to as cathedral glass or plate glass. It was an expensive venture and American glass factories did not manufacture glass with this method until much later in the nineteenth century. Higher quality of glass continued to be imported from France and England until the 1890s. (Roth, 1971) A book published by the Pittsburgh Plate Glass Company (1923), noted there was not a plate glass plant in the United States reaping a profit from the production of glass during the 19th-century.

The perception of color. Color is imparted in glass in two ways. It is produced when electrons in the d orbital of transition metals with certain oxidation states are excited into a higher level from the ground state. This d-d transition has a specific gap length that correlates to a certain wavelength of visible light. Color can also be produced in glass though a transfer of electrons from the metal ion to the ligands in the surrounding glass matrix.

Identification of colorants in glass with analytical techniques. Colorants in glass have been studied by many, using a large array of analytical techniques. Studies on modern and historic glasses were difficult to find because most techniques have been applied to ancient and medieval glass.
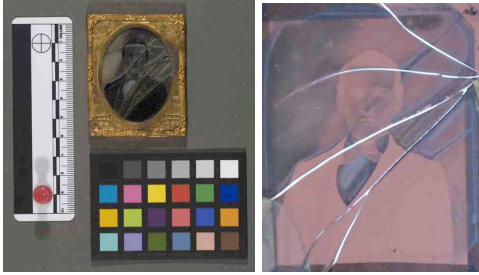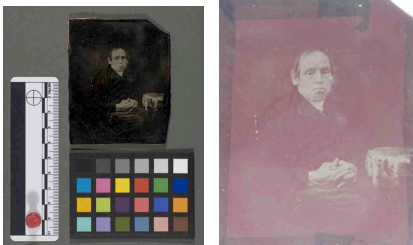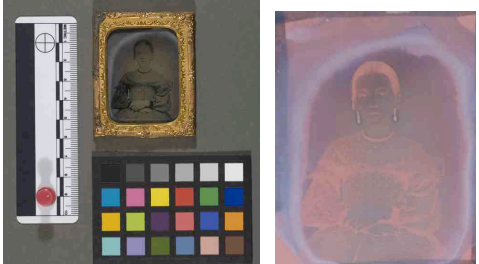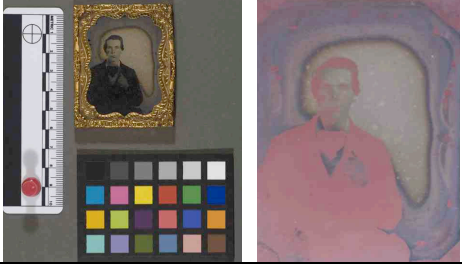
Mass (1999) provides a framework for analyzing glass. In her article she reviews the techniques and provides an extensive bibliography. She states that analysis will answer questions about condition, provenance and fabrication. The transition metals are identifiable with techniques such as x-ray fluorescence (XRF) and SEM-EDS. Cox and Pollard (1977) and Hoffmann (1994) have all studied colorants with XRF. Carmona (2005) and Verita & Basso (1994) used SEM-EDS to determine the composition and color of glass. They described advantages of the SEM capability to selectively sample and therefore exclude inclusions and impurities in the glass.

Scientists have turned to using Ultraviolet/ Visible Light (UV/ Vis) Spectroscopy to study oxidation states in colorants. The SEM and XRF do not easily provide quantitative data or determine oxidation states. UV/Vis spectroscopy has the potential to provide data about the colorants without the need for destructive testing, but has limitations.

2. EXPERIMENTAL
2a: Sample selection
Five ruby ambrotypes were selected for analysis. Two of the ambrotypes (Ambrotype_2 and Ambrotype_4) were from the Winterthur/ University of Delaware Program in Art Conservation study collection. The others (Ambrotype_1, Ambrotype_3, and Ambrotype_5) were purchased by the author, bought on Ebay in the past year. Table 1 is a compilation of images and a description of the five ruby ambrotypes.

Table 1

Reference no. and each image in both reflected and transmitted light	*Description and condition*
Ambrotype_1	Dimension: 2 ½" x 2" x 1/16" (h x w x d) Ninth plate size portrait of a young man. The glass had an orangish red cast in transmitted light. It was purchased on Ebay in poor condition, as the support and cover glass were broken. There was significant deterioration of the image at the edges and also associated with cracks in the cover glass. The paper seal was intact. This sample proved to be valuable as certain SEM required a small sample size for analysis.
Ambrotype_2	Dimension: 3 ¼" x 2 5/8" x 3/32" (h x w x d) Sixth plate size portrait of an old man from the Winterthur/ UD study collection. The color of the glass was darker than the rest and had a violet cast compared to the orange cast of the others. The image surface was in good condition except for abrasions likely caused by the lack of appropriate housing is storage.
Ambrotype_3	Dimension: 2 ½" x 2" x 3/32" (h x w x d) Ninth plate size portrait of a young woman bought on Ebay. The glass has an orangish red color in transmitted light and there was deterioration of the image at the edges. The paper seal was intact.
Ambrotype_4	Dimension: 2 ½" x 2" x 3/32" (h x w x d) Ninth plate size portrait of a young man from the Winterthur/UD collection. The color of the glass was cranberry color in transmitted light. The silver image was deteriorating at the edges.
Ambrotype_5	Dimension: 3 1/8" x 4" x 3/32" (h x w x d) Quarter plate size portrait of a family purchased on Ebay. The color of the glass was reddish purple in transmitted light. The silver image was in good condition with no visual sign of deterioration.

2.b: Methodology
Part I: Visual Interpretation with an ultraviolet light

Ultra-violet Light Examination. All 5 ambrotypes were removed from their packages and viewed with a UVP Inc. Handheld Shortwave/Longwave UV Lamp, Model UVGL-58. Any fluorescence associated with coatings or varnishes was noted.

Part II: Vibrational spectroscopy

Fourier Transform-Infrared (FT-IR) Spectroscopy in reflectance mode. Each ambrotype was studied with FT-IR to identify organic coatings present on the surface. Non-destructive analysis was carried out using a Nicolet Magna-IR 560 ESP with a Nicplan IR microscope. Spectrometer (cooled with liquid nitrogen) with a diffuse reflectance ocular. This allowed readings to be taken directly on the surface of the ambrotypes. In theory, there was a possibility that the silver particles would effectively reflect light to identify the binder and coatings.

Spectra were taken using a polished gold surface background and then the ambrotypes placed and focused directly on the microscope stage. Readings were taken for 120 scans between 4000-650 cm^{-1} and a spectral resolution of 4 cm^{-1}. The generated spectra were brought into OMNIC E.S.P. 1a software and compared to reference library databases.

FT-IR in transmission mode. Each ambrotype was surface cleaned with pressurized air to remove possible contaminants from the surface. Minute representative samples, on the order of micrograms, were removed with a clean scalpel utilizing a Nikon SMZ800 microscope and Sony Trinitron monitor. The samples were placed on a diamond cell and uniformly flattened with a steel roller.

The cell was placed on the microscope stage of the Nicolet Magna-IR 560 Esp. Spectrometer and focused. Spectra were collected in transmission mode from samples on all five ambrotypes. Readings were taken for 120 scans between 4000-650 cm^{-1} and a spectral resolution of 4 cm^{-1}. The generated spectra were brought into OMNIC E.S.P. 1a software and compared to a reference library database.

Raman spectroscopy. Raman spectroscopy did not require sampling and was ideal for analysis of the silver deterioration on the surface of certain ambrotypes. The entire ambrotype was placed on the stage of a Renishaw inVia Dispersive Microscope. The sample was focused on an area of tarnish and excited using a 785nm diode laser (diffraction grating is 1200 lines/mm). The data was collected using Wire 2.0 Software and compared to a natural mineral reference database.

Ambrotype_1 and Ambrotype_4 were studied but it was quickly evident that even under low laser powers, there was a potential to burn the sample. Dark spots were visible under magnification. Spectra were generated at varying laser powers of 0.5%, 0.05% and 0.0001% with photo bleaching.

Part III: Chromatography

Gas Chromatography-Mass Spectrometry (GC-MS). Coatings from Ambrotype_2 and Ambrotype_5 were prepared for analysis with the gas chromatography-mass spectrometer, as analysis using IR instruments was not conclusive. Proper sampling was critical as contamination was possible. GC-MS is often used in addition to FT-IR when studying organic components. Analysis was done using a Hewlett Packard HP 6890 Series GC System equipped with a HP 5973 Mass Selective Detector, a HP 7683 Series Injector, and an HP 59864B Ionization Gauge Controller (calibrated for nitrogen).

Minute samples were removed with a sterilized scalpel and rinsed into a small glass vial with ethanol. This technique gave better results than dry collection because the collodion binder and coating is only 2-6 microns in thickness (McCormick Goodhart, 1990) and was easily lost otherwise. The sample was evaporated and derivitized using MethPrep II reagent. MethPrep II converts carboxylic acids and esters to the methyl ester derivatives. Analysis was carried out using the RTLMPREP method on the GC-MS and run using a Hewlett-Packard 6890 gas chromatograph equipped with a 5973 mass selective detector and 7683 automatic liquid injector. The sample was then analyzed in the mass spectrometer. The generated spectra were compared to a reference database of materials. (include GC conditions)

Part IV: X-ray Methods

Figure 6: Each ambrotype was placed on the stage and analyzed with the portable XRF

X-ray fluorescence (XRF). Using XRF was non-destructive and no sample preparation was needed. All five ambrotypes were placed on the stage of the TRACeR III-V portable XRF spectrometer (Figure 6). The spectrometer had the capability for elemental analysis as low as sodium and utilized a rhenium target x-ray source.

Spectra were generated from the verso of all five ambrotype support glasses. The collection time was 100 seconds, with a 40kV acceleration voltage and an anode current of 2.4 μA. After collection in PXRF32 Key Master Technologies, Inc version 3.6.11 software, the characteristic K_{α} and K_{β} lines as well as certain L_{α} and L_{β} lines identified the elements.

Ambrotype_3 was compared to an object known to be ruby glass in the Winterthur collection using the portable XRF. Both samples were run at the same conditions above but for 600 seconds. This assured that any minor elements would be identified.

Analysis was also carried out using an open structure XRF spectrometer for comparison to the data collected with the portable XRF. Ambrotype_4 was studied with the ArTAX Voltage Tube set to 50 keV, an anode current of 600μA, with a molybdenum target source for 100 seconds. Data was collected in proprietary software of the instrument.

Part V: Ultraviolet and Visible Spectroscopy-absorbance mode
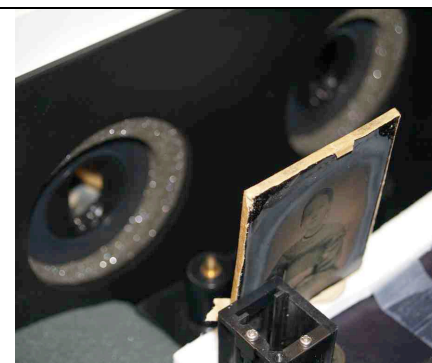
Figure 7: The placement of an ambrotype in the pathway of the beam during analysis with UV/ Vis spectroscopy

The glass was analyzed with a double beam Perkin Elmer Lambda EZ210 Spectrophotometer. A calibration was performed prior to analysis with a holmium oxide standard. Each ambrotype was then surface cleaned on the verso, at one corner, with distilled water. It was placed in the pathway of the sample beam and stabilized on a foam platform and held in place with plastacein putty (Figure 7). The beam passed through areas of glass with no image. Readings were collected between 340-1100 nm with a scan speed of 100 nm/ min. Spectra were plotted by the proprietary software of the instrument for absorbance vs. wavelength.

Part VI: Electron beam methods
Scanning Electron Microscopy-Energy Dispersive Spectroscopy (SEM-EDS). The broken Ambrotype_1 proved to be valuable because it could be studied with the scanning electron microscope. The vacuum chamber on the SEM could hold only up to 3" square and the technique could have been possible without the shattered sample.

A triangular piece from the top right corner was temporarily removed from the object and mounted onto a carbon stub with carbon tape. The sample was heavily tarnished in areas exposed to the environment after the cover glass broke. No further preparation was required. (Figure 8) The triangular piece from Ambrotype_1 was also run in cross-section. It was positioned inside the stub holder and wrapped in copper tape. (Figure 9) In each case, the sample was placed into the chamber and the chamber evacuated.

The SEM functions at magnification of 80X to at least 10,000X, capable of resolving features as small as 0.01 microns. Analysis was performed using a Topcon ABT60 Scanning Electron Microscope equipped with an EDAX 9900 energy-dispersive x-ray analyzer (Philips Electronic Instruments Co.), a cooled SiLi detector, a beryllium window and a tungsten filament gun source. Images were viewed on an Ikegami Monitor.

Black and white backscattered electron images were collected with accelerating voltage of 20 keV and ranging from 500x to 1050x magnification. High incident electron beam with a 20keV accelerating voltage was also used to excite characteristic x-rays from the components of the object. The incident ray penetrates 0.02-1.0 microns into the sample. By using an EDS detector, spot elemental analysis and elemental maps were generated. The EDS detector had the capability of detecting elements in the range of sodium to uranium. All data were collected in Evex NanoAnalysis software.
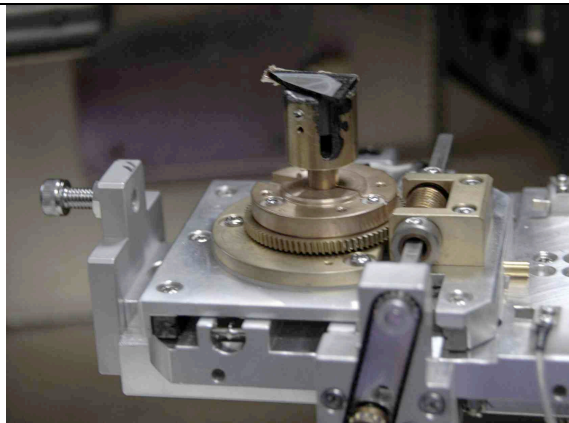

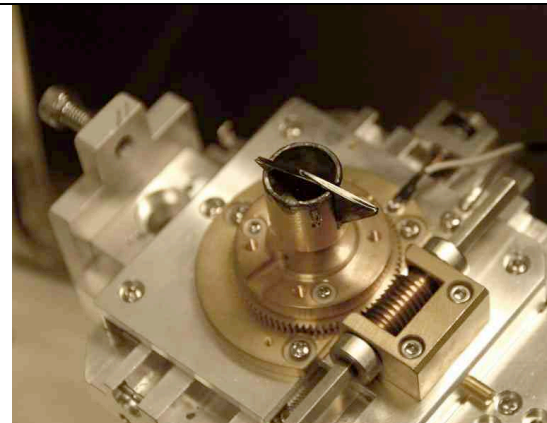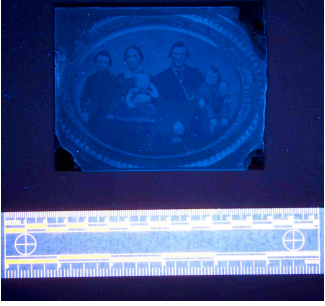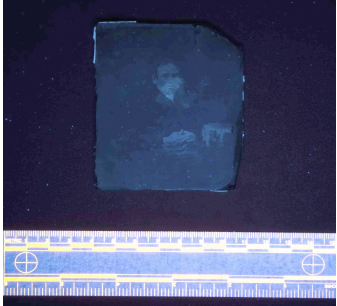| Figure 8: The shard mounted for surface analysis. | Figure 9: The shard mounted for analysis in cross-section |

3. RESULTS

Part I: Visual examination with UV light

Two ambrotypes of the five fluoresced in long wavelength (366nm) UV light. Three showed no discernable fluorescence, alluding to ambrotypes without a final varnish coating. Figure 10 is images of the fluorescent ambrotypes and a table compiling the data.

a.	b.	Name	Fluoresced
		Ambrotype_1	
		Ambrotype_2	X
		Ambrotype_3	
		Ambrotype_4	
Figure 10: Bluish/ white fluorescence of Ambrotype_5 (a) and Ambrotype_2 (b)		Ambrotype_5	X

Part II: Classification of the coatings with FT-IR

The data collected with the FT-IR in reflectance mode contained excessive noise and the software was unable to make a definitive match. The data collected in transmission mode detected the cellulose nitrate binder in all five samples. On the 3 samples that did not fluoresce in UV light, no other components were detected. In the 2 samples that fluoresced, an additional component was detected. Figure 11 shows that in Ambrotype_2 the peak absorbance at 2900 cm^{-1} is amplified, there is a shoulder off the peak at 1250 cm^{-1} and there is an additional peak at the acidic carbonyl site of 1800 cm^{-1}. The reference library was unable to definitively characterize the additional peaks, but it is very similar to a natural resin. Table 2 is a compilation of the molecular stretching bands (sb) and bending bands (bb) for each of the 5 samples.
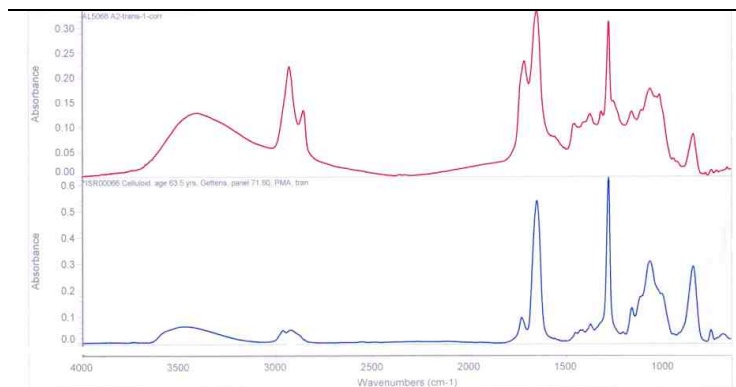

Figure 11: FTIR spectrum of the sample (top) from Ambrotype_2 and a cellulose nitrate reference on the bottom. Notice that there is evidence of an additional component to the cellulose nitrate in the sample.

Table 2

	O-H (sb)	C-H (sb)	N-O (sb)	C-H (bb)	C-O (bb)	N-O (bb)	C=O (sb)	C-O (sb)
Ambrotype_1	X	X	X	X	X	X		
Ambrotype_2	X	X	X	X	X	X	X	X
Ambrotype_3	X	X	X	X	X	X		
Ambrotype_4	X	X	X	X	X	X		
Ambrotype_5	X	X	X	X	X	X	X	X

(include wavenumber ranges)

Part III: Characterization of the coatings with GC-MS

Analysis with the GC-MS revealed a coating with a complex mixture from Ambrotype_2 and is shown in Figure 11. Ambrotype_5 also had a different but equally complex mixture. Peaks for shellac, sandarac, certain fatty acids and other unidentified high molecular weight resin components were detected in the coating of Ambrotype_2, displayed in Figure 12.   The composition of Ambrotype_5 revealed fatty acid components and no resins. There was not sufficient sample for a full characterization of the coating on Ambrotype_5.
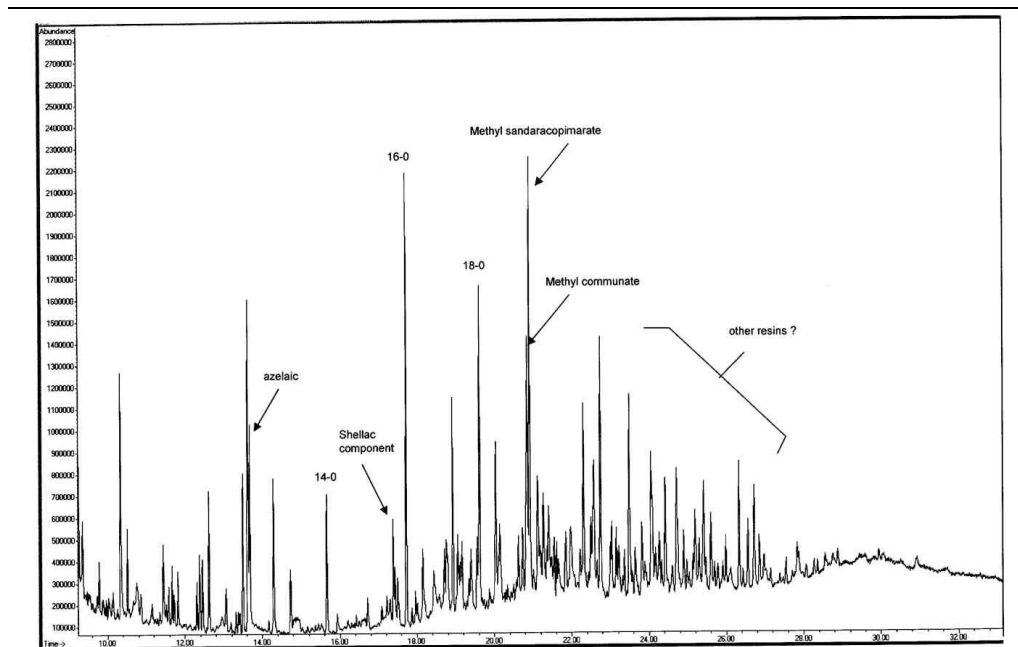
Chromatogram courtesy of Dr. Chris Petersen, Scientific Research and Analysis Lab, Winterthur

Figure 12: The gas chromatogram for Ambrotype_2 revealed a complex mixture of natural resins and fatty acid components.

Part IV: Identification of the colorants in the glass support with XRF
Manganese was identified as the colorant in all five glasses. Four of the glasses also contained additional components of a soda-lime-silica glass matrix. At a scan time of 100 seconds on the portable XRF, one of the lead L_β lines and that arsenic K_α line overlap making conclusive identification of the arsenic peak difficult. In one example, Ambrotype_2, the peak for lead was very strong and distinctive, alluding to a leaded glass matrix. A representative spectrum of a non-lead containing glass from Ambrotype_1 is located in Figure 13. Table 3 is a compilation of the elements detected from each ambrotype using XRF.
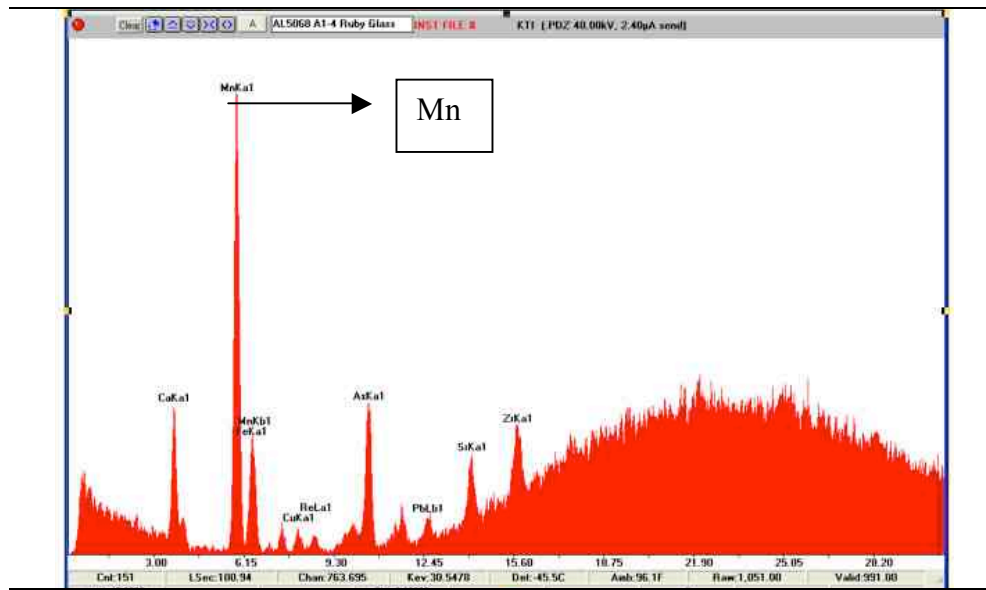

Figure 13: A representative XRF spectrum from Ambrotype_1 showing the presence of manganese.

Table 3 Data collected at 100 seconds with the portable XRF:

	Mn	Ca	As	Pb	Fe	Sr	Zr
Ambrotype_1	X	X	inconclusive	inconclusive	X	X	X
Ambrotype_2	X	X	inconclusive	X		X	X
Ambrotype_3	X	X	inconclusive	inconclusive	X	X	X
Ambrotype_4	X	X	inconclusive	inconclusive	X	X	X
Ambrotype_5	X	X	inconclusive	inconclusive	X	X	X

*Ni, Zn and Cu peaks were detected but are artifacts of the filter on the instrument

Data from the open structure XRF instrument revealed similar compositions to the portable XRF unit. Additional minor elements of Cu, K were identified and Pb was not detected. Table 4 compiles the elements detected.

For comparison, a ruby glass standard from the Winterthur collection was studied. It revealed a very different composition than the ambrotype glasses. Table 5 is a compilation of the elements found in each glass. The ruby glass standard contained gold (Au) and silver (Ag) coloring components and no manganese.

Table 4: Data collected at 100 seconds with the open structure XRF

	Mn	Ca	As	Pb	Fe	K	Cu
Ambrotype_4	X	X	X		X	X	X

Table 5: A direct comparison between one ambrotype and a ruby glass, collected at 600 seconds with the portable XRF

	Mn	Si	Ca	As	Ti	Ba	Zn	Pb	Fe	Au	K	Cu	Sr	Zr	Ag	Sn
Ambrotype_3	X	X	X	X			X	X	X		X	X	X	X		
Ruby glass standard		X	X		X	X	X	X	X	X	X	X	X	X	X	X

Part V: Absorption data for ruby glass with UV/Vis spectroscopy
All five ambrotypes generated similar absorption spectra with UV/Vis spectroscopy. They all absorbed light strongly in the visible region of the electromagnetic spectrum, absorbing in the blue/ green and visible as red. There is also a slight absorbance at the shoulder of each spectrum at approximately 650nm. Table 6 shows the maximum peak absorbance for each glass support. Ambrotype_2 was optically more dense than the rest and the absorption exceeded the sensitivity of the instrument. Figure 14 is an overlay of all 5 peaks, showing their similarities. Although Ambrotype_2 was less transparent and did not generate a peak, it appears to closely follow the other curves.

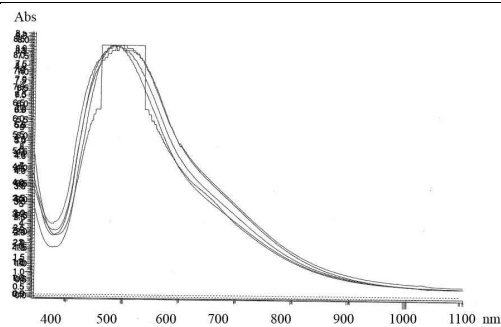| Table 6	
Name	**Wavelength (nm) at peak absorbance**
Ambrotype_1	488
Ambrotype_2	Curve exceeded sensitivity of the instrument
Ambrotype_3	495
Ambrotype_4	498
Ambrotype_5	506

Figure 14: Absorbance vs. wavelength (nm). Overlay of the five absorbance spectra.

Part VI: Surface analysis with SEM-EDS and BSE

Elemental mapping of the surface was carried out with SEM-EDS in four spots. Spot 4 was taken in cross-section. Figure 15 shows the locations of analysis. Table 6 is compilation of the elements found during analysis.
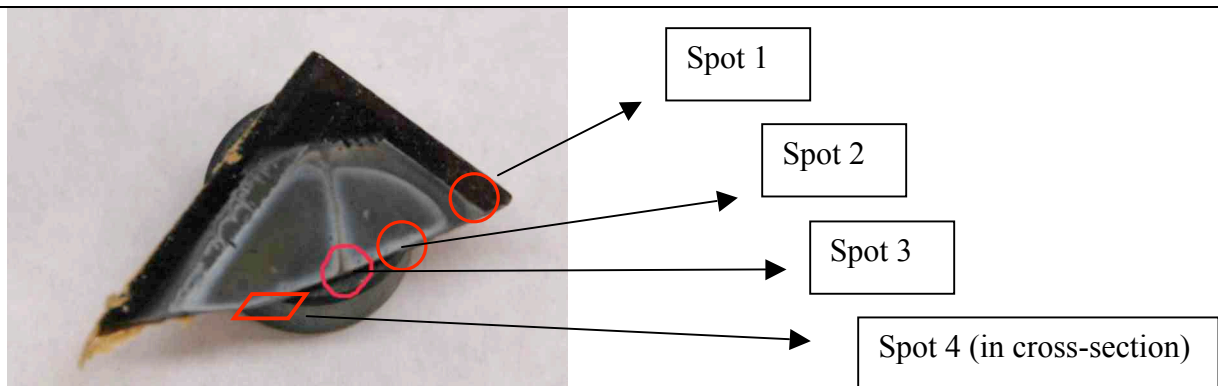

Figure 15: Areas of elemental mapping with SEM_EDS: The edge of the image layer and exposed glass support (Spot 1), the interface of tarnished and image material (Spot 2), the white tarnish (Spot 3) and in cross-section (Spot 4).

Table 6: Elements detected with SEM-EDS

	Ag	Cl	S	Ca	Mn	Si
Spot 1	X	X	X	X	X	X
Spot 2	X	X	X	X	X	X
Spot 3	X	X	X	X	X	X
Spot 4	X			X	X	X

Spot 2, revealed a distinct boundary between areas of white tarnish and areas with no white tarnish, seen in Figure 17. Spot 3, a higher magnification of an area of white tarnish, is shown below with the representative SEM-EDS map. The BSE image from the spot, displayed in Figure 18, revealed large cubic crystals above the background. Elemental mapping located chlorine (yellow), seen in Figure 19, at these crystals. In an overlay of the maps in Figure 20, the crystals also clearly contained silver (red). It is inferred from the data that silver chloride (AgCl) salts stood above a silver sulfide (Ag_2S) background. Sulfur was detected in the background and is evident by light blue pixels. The Ca, Mn and Si were all components from the underlying glass support.
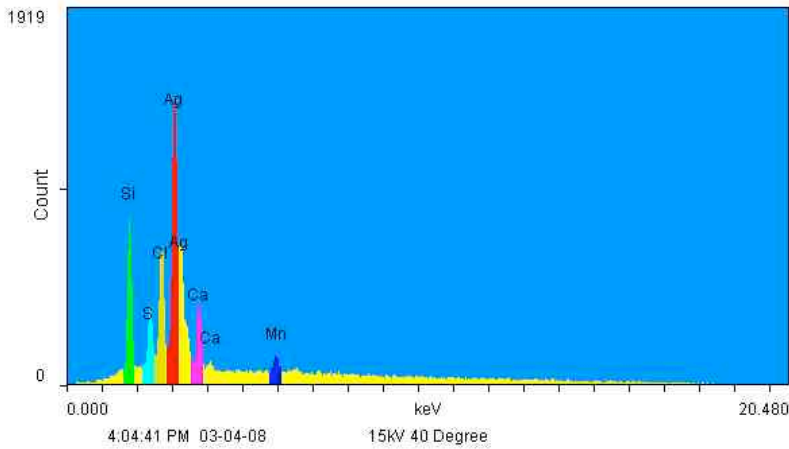
Element	Color
Ag	red
Si	green
Cl	yellow
Ca	pink
Mn	dark blue
S	light blue

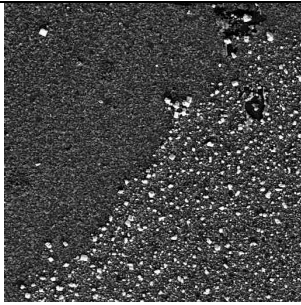Figure 16: SEM-EDS elemental map and a color chart generated from Spot 3

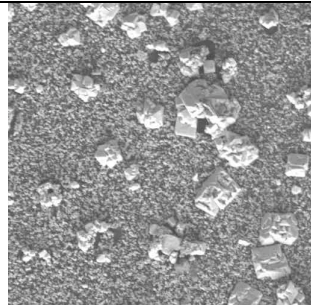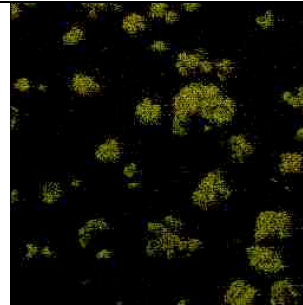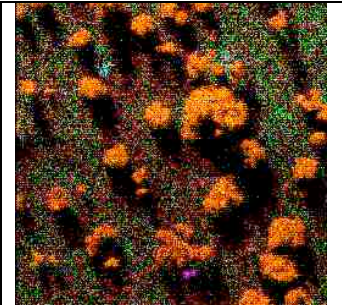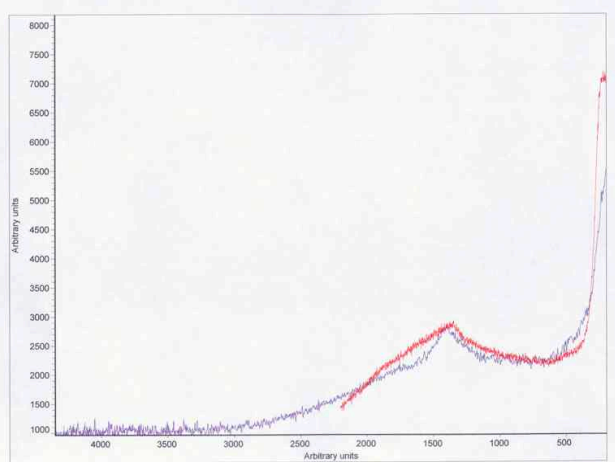| Figure 17: BSE image from Spot 2 showing the distinct line between areas of white tarnish (right) and areas not tarnished (left), 500X | Figure 18: BSE image of surface at Spot 3 in a white tarnished area, 750X | Figure 19: SEM-EDS map from Spot 3 for chlorine (yellow). It is concentrated at the crystals, 750X | Figure 20: SEM-EDS mapping on all six elements. The crystals appear orange because of silver (red) and chlorine (yellow), 750X |

Part VII: Surface analysis with Raman spectroscopy

The spectra generated from the surface analysis of Ambrotype_1 and Ambrotype_4 matched the spectrum for acanthite, a silver sulfide mineral. An overlay of a spectrum taken in the tarnished area of Ambrotype_4 (red) and an acanthite reference (purple) is displayed in Figure 21.

Figure 21: Raman spectra from Ambrotype_4 (red) overlaid with the reference spectra of acanthite (purple).

4. DISCUSSION

4a. Coatings on ruby ambrotypes

Both FTIR and GC-MS revealed evidence for a varnish coating containing natural resin components. Both spectra for the GC-MS revealed a complex and somewhat confusing varnish coating. There were peaks from shellac, a common coating used historically, and also peaks coming from components of a sandarac resin, also used historically. However, there is no known mention of using shellac and sandarac in tandem. Both resins are components of spirit varnishes mixable in polar solvents but appear to have been combined with a fatty acid component, possibly a drying oil. Also, certain other unknown resin peaks were noted suggesting the presence of a complex mixture.

It is possible that the coating was an oil resin varnish which has hardened through a polymerization of oils. This was a sandarac resin and linseed oil varnish used into the 19th-century for industry. (Baade, 2008) These coatings were slow cooked under high heat and applied to a surface when cooled. The data are inconclusive since no additional fatty acids characteristic of oils were detected in these tests.

Primary texts were consulted to seek information regarding 19th-century photographic oil resin varnishes. Photographic catalogs sold proprietary ambrotype varnishes, boasting the effectiveness of these secret solutions and revealing nothing of their compositions. (Anthony's catalog, 1857) It is also known that ambrotypists made their own varnishes, following recipes outlined in journals or by word of mouth (Humphrey's Journal, 1857).

Regardless of the ingredients in the varnish, it protected the image from deterioration as the three without coatings show signs of silver tarnish. It was not discovered why ambrotypists did not coat every plate, but it was mentioned they did not like the appearance of a coated image (Burgess, 1858). It appears the aesthetic qualities of the photograph were chosen instead of protecting the image from damage.

From a conservator's perspective, once tarnish is evident it is not reversible. There is no current agreement for treating issues related to image deterioration and further discussion is beyond the scope of the study.

4b. Silver tarnish on ruby ambrotypes

Both SEM-EDS and Raman spectroscopy detected silver sulfide tarnish. The absence of chlorides detected on the surface is not surprising as the peaks were below the cutoff filter of the Raman spectrometer. They would have undoubtedly been detected given the proper instrumental conditions.

When silver is exposed to pollutants and gases in the environment it tarnishes. The mechanism is initiated in an oxidizing environment when an oxide of silver is formed at the surface. In the presence of water, these oxides provide an electrostatic potential that promotes the penetration of corrosive sulfide and chloride ions to attack the structure. (Nishimura, 2008)

Figure 22: The white haze is due to the scattering of light by silver chloride crystals. The reddish orange tarnish is silver sulfide interference colors.

Reducible sulfur is present in the atmosphere from volcanic eruptions as well as generated in combustion reactions. Chlorine components are also prevalent in the environment. They are generated industrially in combustion reactions of plastics, leaded fuels, and coal. It is a common component of particulate matter, especially in areas next to the ocean but also in areas inland.

Photographic image silver is especially vulnerable to attack. Due to the small size of silver grains, there is a large surface area for reactions to occur. Also, the silver particles above the collodion binder are exposed. (McCormick-Goodhart, 1990, 263) In the ambrotype studies it appeared that the scattering of light by small silver chloride crystals caused the whitish haze. The colored tarnish was explained by interference from thin layers of silver sulfide. Figure 22 is a photomicrograph of the tarnish on Ambrotype_1. The presence of sulfides confirms research about tarnish published by others on the surface of cased objects. Image deterioration characterized as chloride crystals is however sparse and warrants additional research. A discussion on the significance of chloride contamination to cased objects is just beginning. Silver chloride salts are sensitive

to light and the implications of this deterioration will need to be addressed in the future.

4c. *The colorants for the ruby ambrotype glass support*

Although known as *ruby ambrotypes*, none of the 5 samples were made on a traditional ruby glass. The reddish color was not made with a precipitate of silver or gold, but colored by a complex of manganese in the glass matrix.

A recipe book from 1899 (Biser) provided a number of recipes with manganese in combination with the other metals found using XRF. The recipes for *black glass* best matched the composition. Refer to Appendix 1 for a list of recipes. In reflecting back to an 1857 photographic catalog, the word "purplish-black" glass now seems very appropriate.

Manganese is one of the oldest colorants for glass, dated to as early as 1400 BCE. Chemically, the trivalent manganese (Mn^{3+}) ion produced in a low melt and oxidizing environment, complexes with its surroundings to form a purple glass with a potential to produce a range of colors from reddish to more blue. (Weyl, 1976) The surrounding matrix and concentration are influential in determining the perceived color. The divalent manganese (Mn^{2+}) also plays a role in the color of the glass, although it is much weaker and forms complexes visible in the brown region of the spectrum. (Weyl, 1976)
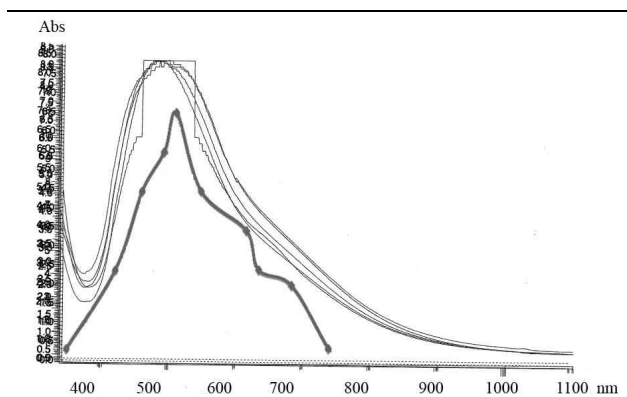

Figure 23: A resemblance between the ruby ambrotype spectra and a reference spectrum for glass with manganese in the trivalent state.

The peak absorbance of all five ambrotype glasses matched published data for a complex of glass containing trivalent manganese (Mn^{3+}). Green and Hart (1987) studied mid 16th-century glass shards with a UV/Vis spectrometer. Presented were absorption spectra for a red glass containing Mn^{3+} in an octahedral state occurring at λ_{max}=470-520nm. Also, an absorbance spectrum of trivalent manganese glass was found (Fedotieff, 1924) and overlaid over the five ambrotype spectra from the study, Figure 23. The resemblance is evident and even the small absorbance at the shoulder is present in all the curves.

5. CONCLUSION

In this small sample of ruby ambrotypes, features not previously discussed in the literature were addressed. The primary colorant in the ruby glass was found to be manganese. The presence of an intact surface coating seems to have protected the image from silver tarnish. When the surface coating was not present, silver tarnish developed in

the image over time. The chemical composition of image tarnish found on the ruby ambrotypes was similar to that reported in previous studies of cased-photographic objects. Larger studies of ruby ambrotype images will be necessary to confirm these preliminary findings. The importance of ambrotypes as historical documents of a time period is certain and their preservation is a priority. The implications for conservation treatment and preventive measures are not formed, but are identified as areas of essential study in the future.

6. ACKNOWLEDGEMENTS

7. REFERENCES

Anthony's bulletin of photography, invention and improvement. 1857. New York, NY: Holman (printer). [Hagley Museum and Library, Wilmington, DE]

Baade, B. 2008. Personal Communication. Winterthur/ University of Delaware, Newark, DE.

Barger, S. et al. 1984. Protective surface coatings for daguerreotypes. *Journal of the American Institute for Conservation*. 24 (1): 40-52.

Barger, S. 1989. Characterization of corrosion products on old protective glass, especially daguerreotype cover glasses. *Journal of Materials Science* 24: 1343-1356.

Barger, S. et al. 1982. The cleaning of daguerreotypes: comparison of cleaning methods. *Journal of the American Institute for Conservation*. 22 (1): 13-24.

Biser, B. 1899. *Elements of glass making*. Pittsburgh, PA: Glass and Pottery Publishing Co.

Burgess, N.G. 1858 4th ed. *The photograph and ambrotype manual: a practical treatise*. New York, NY: Wiley and Halsted.

Carmona, N., M.A. Villegas and J.M. Fernandez Navarro. 2005. Study of glasses with grisailles from historic stained glass windows of the cathedral of Leon (Spain). *Applied Surface Science* (252) 16: 5936-5945.

Centano, SA, T. Meller and N. Kennedy 2008. The daguerreotype surface as a SERS substrate: characterization of image deterioration on plates from the studio of Southworth & Hawes. *Journal of Raman Spectroscopy*.

Cox, G.A. and A.M. Pillard. 1977. X-ray fluorescence analysis of ancient glass: the importance of sample preparation. *Archaeometry*, 19 (1) : 45-54.

Daffner, L et al. 1996. Investigation of a surface tarnish found on 19th-century daguerreotypes. *Journal of the American Institute for Conservation*, 35 (1) :9-21

Derrick, M., and D. Stulik, and J. Landry. 1999. *Infrared spectroscopy in conservation science*. Los Angeles, CA: The Getty Conservation Institute.

DiPietro, G and F. Ligterink. 2002. Silver-mirroring edge patterns: diffuse-reaction models for the formation of silver-mirroring on the silver gelatin glass plates. *Journal of the American Institute for Conservation*, 41 (2) :111-126.

Fedotieff, P. and A. Lebedeff. 1924. Über die absorptionspektra van gefärbten gläsern. *Zeitschrift für anorganiche und allgemeine Chemie*. 134 (1): 87-101.

Green, L.R. and F. A. Hart. 1987. Colour and chemical composition in ancient glass: an examination of some Roman and Wealden glass by means of ultraviolet-visible-infrared spectrometry and electron microprobe analysis. *Journal of Archaeological Science* 14: 271-282.

Haist, G. 1979. *Modern photographic processing*. New York, NY: John Wiley and Sons.

Hatchfield, P. 2002. *Pollutants in the museum environment*. London, England: Archeotype Publications.

Hoffmann, P. 1994. Analytical determination of colouring elements and of their compounds in glass beads from graveyards of the Merowings time. *Fresenius J. Anal Chem* 349: 320-333.

Humphrey's Journal. 1857. Positive Collodion Process. *Humphrey's Journal* 9(4).

Lloyd, J. 1963. *Stained glass in America*. Jenkintown, PA: Foundation Books.

Mass, J. 1999. Instrumental methods of analysis applied to the conservation of ancient and historic glass. In *Conservation of glass and ceramics: research, practice and training*. Ed. N.H. Tennent et al. London, UK: James and James.

McCabe, C. 1991. Preservation of 19th Century negatives in the National Archive. *Journal of the American Institute of Conservation* 30(1):41-73.

McCabe, C et al. 2005. *Coatings on Photographs*. Washington, D.C.: American Institute for Conservation.

McCormick Goodhart, M. 1989. *Topics in photographic preservation vol. 3*. Research in collodion glass plate negatives: coating thickness and FTIR identification of vanishes. Washington, D.C.: AIC.

McGlinchey, C and C. Maines. 2005. Chemistry and Analysis of coating materials. In *Coatings on Photographs*. Ed. C. McCabe et al. Washington, D.C.: American Institute for Conservation.

McMormick Goodhart, M. 1992. Glass corrosion and its relation to image deterioration in collodion wet-plate negatives. *Conference Proceedings: The Imperfect Image; Photographs Their Past, Present and Future.* Windermere, Cumbria, England. 256-265.

McMormick Goodhart, M. 1992. An analysis of the image deterioration in wet-plate negatives from the Mathew Brady Studios. *Conference Proceedings: The Imperfect Image; Photographs Their Past, Present and Future.* Windermere, Cumbria, England. 245-255.

McCormick-Goodhart, M. 1990. The multilayer structure of tintypes. *ICOM Committee for Conservation preprints*. 9th Triennial Meeting, Dresden, GDR. Paris: ICOM. 1:262-267.

Moor, I. 1976. The ambrotype—research into its restoration and conservation Part 1. *The paper conservator*. 1: 22-25.

Moor I. 1976. The ambrotype—research into its restoration and conservation Part 2. *The paper conservator* 2: 36-43.

Newhall, B. 1958. Ambrotype, a short and unsuccessful career. *Image*. International Museum of Photography at the George Eastman House. 7(8): 171-177.

Nishimura, D. 2008. Personal communication. Image Permanence Institute. Rochester, NY.

Osterman, M. 2007. Personal communication. Scully & Osterman Studio and George Eastman House, Rochester, NY.

Osterman, M. and G. Romer. 2007. History and evolution of photography. In *Focal Encyclopedia of Photography 4th edition*. Ed Peres, M. et al. Amsterdam: Elsevier.

Penichon, S. 1999. Differences in image tonality produced by different toning protocols for matte collodion photographs. *Journal of the American Institute for Conservation*, 38 (1) :124-143.

Perron, J. 1989. *Topics in photographic preservation vol. 3*. The use of FTIR in the study of photographic materials. Washington, D.C.: AIC.

Pittsburgh Plate Glass Company. 1923. *Glass: history, manufacture and its universal application*. Pittsburgh, PA: Pittsburgh Plate Glass Company.

Reilly, J. 1986. *Care and identification of 19th century photographic prints*. Rochester, NY: Eastman Kodak Co.

Roth, R. 1971. Windows and window glass in the United States before 1860. Corning, NY: Corning Museum of Glass.

Schimmelman, J. 2002. *American photographic patents the daguerreotype & wet plate era 1840-1880*. Nevada City, CA: Carl Mautz Publishing.

Sloan, J. 1993. *Conservation of stained glass in America*. Wilmington: DE: Art in Architecture Press.

Stambolov, T. 1966. Removal of corrosion on an 18th-century silver bowl. *Studies in Conservation*. 11(1) 37-44.

Swan, A. et al. 1979. Daguerreotypes: a study of the plates and the process. *Scanning Electron Microscopy*. 1: 411-23.

Verita, M and R. Basso. 1994. X-ray microanalysis of ancient glassy materials: a comparative study of wavelength dispersive and energy dispersive techniques. *Achaeometry*. 36(2) 241-251.

von Waldthausen, C. Selective annotated bibliography of articles on coatings, fading and permanance. Andrew W. Mellon workshop. Fotorestauratie Atelier CC von Waldthausen. Amsterdam, the Netherlands: Unpublished transcript.

Weaver, G. 2008. A guide to fiber-base gelatin silver print condition and deterioration. Advanced Residency Program, George Eastman House International Museum of Photography and Film, Image Permanence Institute.

Weyl, W.A. 1976. *Coloured Glass*. Sheffield, England: Society of Glass Technology.

Appendix 1: Black Glass Recipes

Common Glass:

Green Cullet………………100	**Manganese………………8**
Soda………………………..38	Oxide of Iron……....……..6
Lime………………………18	Pulverized coke………….4
Arsenic…………………….2	

Fine Glass:

Sand………………………..100	Oxide of copper…………10
Potash……………………..36	Oxide of iron…………….10
Lime………………………..13	**Manganese ...……………10**
Zaffre………………………10	

Sand………………………100	Oxide of copper………….4
Potash……………………...15	Oxide of iron……………..4
Soda………………….24	**Manganese………………5**
Lime………………………18	Zaffre…………………….2

Biser, B. 1899. *Elements of Glass and Glassmaking*. Pittsburgh, PA: Glass and Pottery Publishing Co.

Appendix 2: Additional Bibliography

Brill, T.1980. *Light it's interaction with art and antiquities*. New York, NY: Plenum Press.

Clark, S. 1998. The conservation of wet collodion positives. *Studies in Conservation*. 43: 231-241.

Crawford, W. 1979. *The keepers of light*. Dobbs Ferry, NY: Morgan and Morgan.

Derrick, M. 1989 spring. Fourier infrared spectral analysis of natural resins used in furniture finishes. *Journal of the American Institute for Conservation*, 28 (1) :43-56.

Feller, R., N. Stalow and E. H. Jones. 1985. *On picture varnishes and their solvents*. Washington, D.C.: National Gallery of Art.

Horie, C.V. 1987. *Materials for conservation*. Amsterdam: Elsevier Butterworth Heinemann.

Mills, J. and R. White. 1994. *The Organic Chemistry of Museum Objects*. Oxford, UK: Butterworth Heinemann.

Newton, R and S. Davison. 1989. *Conservation of Glass*. Oxford, UK: Butterworth Hainemann.

Odegaard, N, S. Carroll, and W. S. Zimmt. 2005. *Material characterization tests for objects of art and archeology*, 2d ed. London, UK:.Architype publications.

Searles, E. *Topics in photographic preservation vol. 8*. Investigation into the pollution of the silver bath. Washington, D.C.: AIC.

Scholes, S. 1916. The American pressed and blown glass tableware industry. *Journal of the society of chemical industry* 35: 515-520.